Optica Applicata, Vol. XIV, No. 1, 1984

Correlation of optical and generation properties of YAG:Nd^{3+} rods*

Jerzy Czeszko, Sławomir Kaczmarek

Institute of Quantum Electronics, Military Technical Academy, 01–489 Warszawa-Bemowo, Poland.

1. Introduction

Optical investigations of the quality of YAG:Nd^{3+} laser rods with the system of Twyman-Green interferometer do not give complete information as to their application into laser systems, especially in selection of the dye Q-switch.

This work presents the results of optical investigations of YAG:Nd^{3+} rods performed for 145 Polish rods of 3 mm diameter and 50 mm length. These investigations included the Twyman-Green interferometric measurements and determination of the features of a multimode generation for the giant pulse generation.

2. Interferometric investigations

The investigations were made to verify the optical quality of YAG:Nd^{3+} single crystals, from which the laser rods were cut off. Typical interferograms of YAG single crystals and photographs with light passing across are presented in photos (Figs. 1–3).

Rods were cut off from the regions of equal distribution of interference fringes of the same direction and density. The quality of mechanical working was measured in the system of Mach-Zehnder interferometer, where the mutual parallelism of rod ends and their flatness were measured. The rods with the parallelism less than 5″ and the flatness greater than $\lambda/20$ were omitted. The optical quality of YAG rods were determined from the number of interference fringes on the unit length of rod in the system of Twyman-Green interferometer.

The results of optical quality measurements for some of the rods investigated are presented in Table 1. Typical interferograms of YAG rods are presented in photographs (Figs. 4–6).

---

* This paper has been presented at the European Optical Conference (EOC'83), May 30–June 4, 1983, in Rydzyna, Poland.

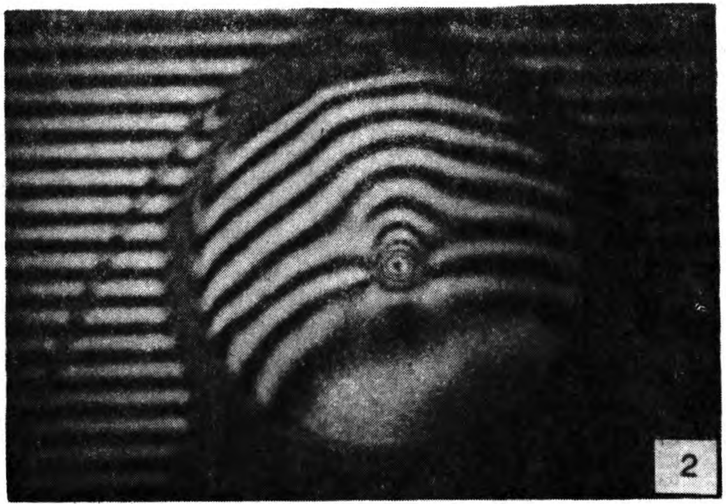

Fig. 1. The interferogram of YAG single crystal for zeroth background of interferometer

Fig. 2. The interferogram of YAG single crystal for compressed background of interferometer

Fig. 3. The image of YAG single crystal with light passing across the crystal

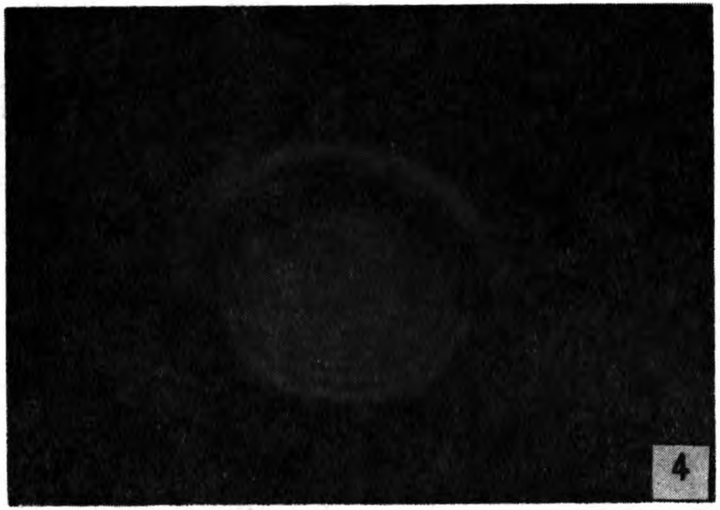

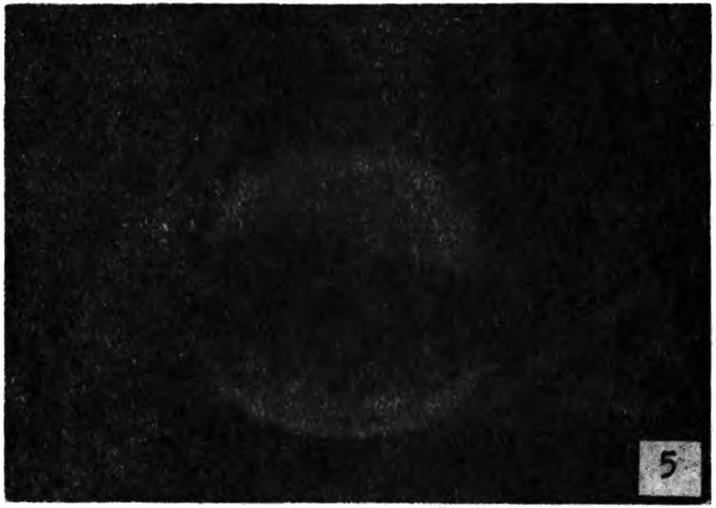

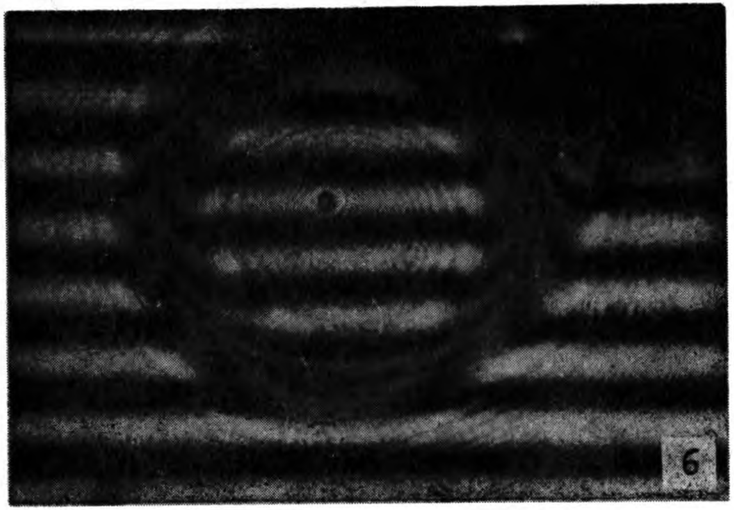

Fig. 4. The interferogram of YAG: Nd^{3+} rod for the zeroth background of interferometer with zero-order fringes on the object

Fig. 5. The interferogram of YAG: Nd^{3+} rod for the zeroth background of interferometer with the one fringe on the object

Fig. 6. The interferogram of YAF: Nd^{3+} rod for the compressed background of interferometer (6-th order of interference) which shows the quality of optical working

Table 1

No. of a rod	17	63	65	82	86	87	88	89	90	91	92	93	97	98	99
No. of fringes on the unit length	0	0.2	0	0.4	0.2	0.4	0	0.1	0	0.2	0	0.2	0.4	0.4	0.2
No. of a rod	101	102	103	104	105	106	107	108	123	124	126	131	135	141	81
No. of fringes on the unit length	0.4	0	0.2	0.4	0	0.4	0.2	0.2	0.2	0.4	0.4	0.4	0.2	0.4	0.8
No. of a rod	80	79	78	77	72	100									
No. of fringes on the unit length	0.2	0.4	0.4	0.4	0.4	0.5									

3. The measurement of absorption coefficient

The absorption coefficient (ϱ) was determined for some output mirrors by dynamical measurement of rod parameters at the beginning of generation [1]. The transmissions of these mirrors were: $11^{0}/_{0}$, $15^{0}/_{0}$, $48^{0}/_{0}$, $60.9^{0}/_{0}$ and $69^{0}/_{0}$.

The relationship between the absorption coefficient (ϱ) and the coefficient of laser amplification (k) is the following [1]:

$$k = \varrho - \frac{1}{l}\ln T_f - \frac{1}{2l}\ln R_1R_2 \tag{1}$$

where: l – active length of laser rod,

T_f – transmission of plastic foil nonlinear absorber for a neodymium laser,

R – reflection coefficient of mirrors.

The absorption coefficient can be found from a ratio of the pumping energy E_p to output energy while the threshold energy of generation is to be found as indicated in the following formula [1]:

$$\frac{E_p}{E_{\mathrm{th}}} = 1 - \frac{1}{2\varrho l}\ln R. \tag{2}$$

From the dependence of E_p on $\ln R$ we can calculate the absorption coefficient ϱ, for YAG:Nd^{3+} rod. The dependence of threshold energy on the exit losses is as follows [1]:

$$(E_p - E_{\mathrm{th}}) = k_r \tan\alpha, \tag{3}$$

$$k_r = \frac{1}{2l}\ln\frac{1}{R_1R_2}. \tag{4}$$

For the mirrors applied here we have:

$$k_{r_1}(R_z = 0.889) = \frac{1}{8.6\,\mathrm{cm}}\ln\frac{1}{0.999\times 0.889} = 0.014\,\mathrm{cm}^{-1},$$

$$
\begin{aligned}
k_{r_2}(R_z = 0.845) &= \frac{1}{8.6\text{ cm}}\ln\frac{1}{0.999\times 0.845} = 0.019\text{ cm}^{-1},\\
k_{r_3}(R_z = 0.52) &= \frac{1}{8.6\text{ cm}}\ln\frac{1}{0.999\times 0.52} = 0.076\text{ cm}^{-1},\\
k_{r_4}(R_z = 0.391) &= \frac{1}{8.6\text{ cm}}\ln\frac{1}{0.999\times 0.391} = 0.109\text{ cm}^{-1},\\
k_{r_5}(R_z = 0.302) &= \frac{1}{8.6\text{ cm}}\ln\frac{1}{0.999\times 0.302} = 0.139\text{ cm}^{-1}.
\end{aligned}
\tag{5}
$$

Let us examine the measurement of ϱ, say for instance for rod of number 126. Table 2 contains the results of output energy measurements for this rod for a different pumping energy and output mirror transmission.

Table 2

E_p [J]	E_{out} [mJ] $T_z = 11\%$	E_{out} [mJ] $T_z = 48\%$	E_{out} [mJ] $T_z = 60.9\%$	E_{out} [mJ] $T_z = 69\%$	U_p [V]
2.02	1.67	—	—	—	600
2.37	3.11	1.67	—	—	650
2.75	4.23	4.52	1.13	—	700
3.15	5.09	6.78	2.83	1.41	750
3.59	6.78	9.89	5.64	3.96	800
4.05	8.47	13.56	8.76	7.06	850
4.54	9.61	17.23	12.71	10.17	900
5.06	11.30	21.75	16.67	15.54	950

A plot of $E_p = f_2(E_{\text{out}})$ is a straight line. The value of E_{th} for the individual transmissions is found by the least squares method (Table 3).

Table 3

T_z	11%	48%	60.9%	69%
E_{th} [J]	1.45	2.15	2.7	3.02
k_r [cm^{-1}]	0.014	0.076	0.109	0.139

A plot of $E_{\text{th}} = f_1(E_{\text{out}})$ is a straight line too, and its slope gives the value of ϱ. Applying also the least squares method, we have $\varrho = 0.092$. In this way we have measured the values of absorption coefficient ϱ for 145 Polish rods. It has been noticed that among the rods investigated there are such for which the value of $E_{\text{mult gen}}$ does not depend on the angle of rod rotation with respect to optical axis, for example, for the rod No. 130, and such rods which demonstrate this dependence, for example, rod No. 115.

Hence, for the next measurements the angle of rod rotation has been optimized with regard to the maximal energy of multimode generation.

4. Estimation of the quality of the Q-switch elements

To the bleachable dye Q-switch we applied the plastic foil nonlinear absorber for a neodymium laser (FNA 1064), which was stuck into two parallel flat plates from the BK-7 glass. Transmission mirror was put on one plate and antireflection layer on the other one. The dye, applied here, is optically and chemically resistant. We have obtained the time of giant pulse Q-switching equal to 7–8 ns. The FNA stands about 40,000 pulses (the details concering the dye and FNA will be presented in the work by Konarski [2]). The technology of production of the Q-switch requires the ideal purity conditions.

The parameter which characterizes the FNA and mirror is their transmissions for $\lambda = 1.064\ \mu m$.

We have prepared FNA with 25–55$^0/_0$ transmission and mirrors with 45–79$^0/_0$. The Q-switch parameters, their selection into YAG : Nd^{3+} rods, generation properties for some rods are shown in Table 4.

5. Selection of the Q-switch into the rod

It is necessary to examine the influence of FNA transmission, T_f, mirror transmission, T_z, and resultant transmission, T_w, on the obtained energetic characteristics of lasers heads. The following characteristics have been determined: E_{th} of giant pulse generation vs. T_w (Fig 7), E_{out} of giant pulse generation vs. T_w

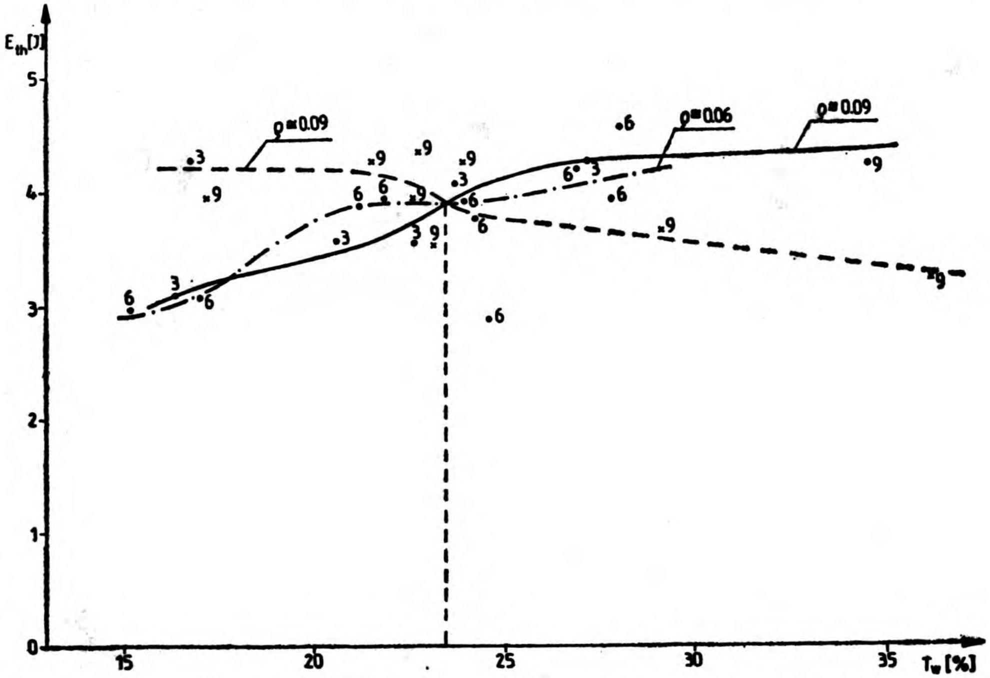

Fig. 7. The dependence of threshold pumping energy E_{th} on the resultant transmission

Table 4

No.	No. of a rod	$T_z[\%]$	$T_f[\%]$	$T_w[\%]$	U_1 [V]–U_2 [V] (E_1 [J]–E_2 [J])	ΔU [V]	E_{out}[mJ]	ϱ	Number of interference fringes on the unit length
1	2	3	4	5	6	7	8	9	10
1	17	61.2	37	24.3	870–1000 (4.24–5.61)	130	6.8	0.003	0
2	63	63	47	21.6	870–990 (4.24–5.49)	120	4.2	0.088	0.1
3	65	65	47	34.6	870–960 (4.24–5.16)	90	5.0	0.021	0
4	82	55	50	21.9	840–1000 (3.95–5.61)	160	7.0	0.062	0.2
5	86	63	42	20.6	800–915 (3.58–4.69)	115	4.6	0.024	0.1
6	87	59.6	37	21.2	830–885 (3.86–4.39)	55	4.6	0.063	0.2
7	88	63	40.6	22.7	800–890 (3.58–4.44)	90	7.7	0.031	0
8	89	61.2	37	24.3	820–910 (3.77–4.64)	90	4.6	0.065	0.05
9	90	63	37	24.7	720–850 (2.9–4.05)	130	5.0	0.057	0
10	91	60.5	37	24.2	750–865 (3.15–4.19)	115	5.0	0.040	0.1
11	92	60	39.5	24.0	840–940 (3.95–4.95)	100	4.4	0.056	0
12	93	58.6	37	23.8	855–910 (4.09–4.64)	55	5.6	0.038	0.1
13	97	61	39.5	24.2	760–860 (3.24–4.14)	100	4.5	0.049	0.2

1	2	3	4	5	6	7	8	9	10
14	98	72	50	36.3	760–860 (3.24–4.14)	100	4.5	0.092	0.2
15	99	63	40.6	22.7	730–825 (2.98–4.79)	95	4.2	0.053	0.1
16	101	69	39.7	29.2	810–910 (3.67–4.64)	100	5.6	0,078	0.2
17	102	61.5	40.6	16.4	740–830 (3.07–3)86)	90	5.1	0.022	0
18	103	69	39	23.2	780–870 (3.41–4.24)	90	7.7	0.092	0.1
19	104	69	39	15.2	730–820 (2.98–3.77)	90	4.5	0.056	0.2
20	105	55	40.5	17.0	740–860 (3.07–4.14)	120	4.2	0.065	0
21	106	63	40.6	20.8	820–925 (3.77–4.79)	105	4.8	0.045	0.2
22	107	69	43.2	29.3	800–890 (3.58–4.44)	90	4.5	0.046	0.1
23	108	69	39	27.8	840–955 (3.95–5.10)	115	4.0	0.059	0.1
24	123	55	40.5	16.8	880–1000 (4.34–5.61)	120	8.5	0.030	0.1
25	124	44	39	17.3	840–1000 (3.95–5.61)	160	7.0	0.117	0.2
26	126	55	50	22.8	880–1000 (4.34–5.61)	120	6.7	0.098	0.2
27	131	59.2	37	24.0	870–980 (4.24–5.38)	110	7.0	0.096	0.2
28	135	55	50	22.7	840–980 (3.95–5.38)	140	7.9	0.099	0.1
29	141	61	50	27.2	870–1000 (4.24–5.61)	130	5.0	0.037	0.2

03	81	52	50	26.2	880–1000 (4.34–5.61)	120	4.9	0.040	0.4
31	80	52	50	26.2	840–990 (3.95–5.49)	150	6.4	0.044	0.1
32	79	47	45.5	21.6	875–1000 (4.29–5.61)	125	5.2	0.079	0.2
33	78	55	50	28.1	890–1000 (4.44–5.61)	110	5.0	0.058	0.2
34	77	52	37	19.8	875–1000 (4.29–5.61)	125	6.8	0.041	0.2
35	72	61	43.8	27.0	870–950 (4.24–5.06)	80	5.1	0.062	0.2
36	100	69	47	32.4	830–920 (3.86–4.74)	90	5.7	0.323	0.25

(Fig. 8), E_{th} of giant pulse generation vs. T_f (Fig. 9), the area width of giant pulse generation, ΔU, vs. T_f and $E_{\mathrm{mult\ gen}}$ of multimode generation vs. T_z.

Figure 7 shows the dependence of threshold pumping energy, E_{th}, on the resultant transmission. For this purpose the results shown in Table 4 for different values of absorption coefficient ϱ ($\varrho \cong 0.03$, 0.06, and 0.09) have been

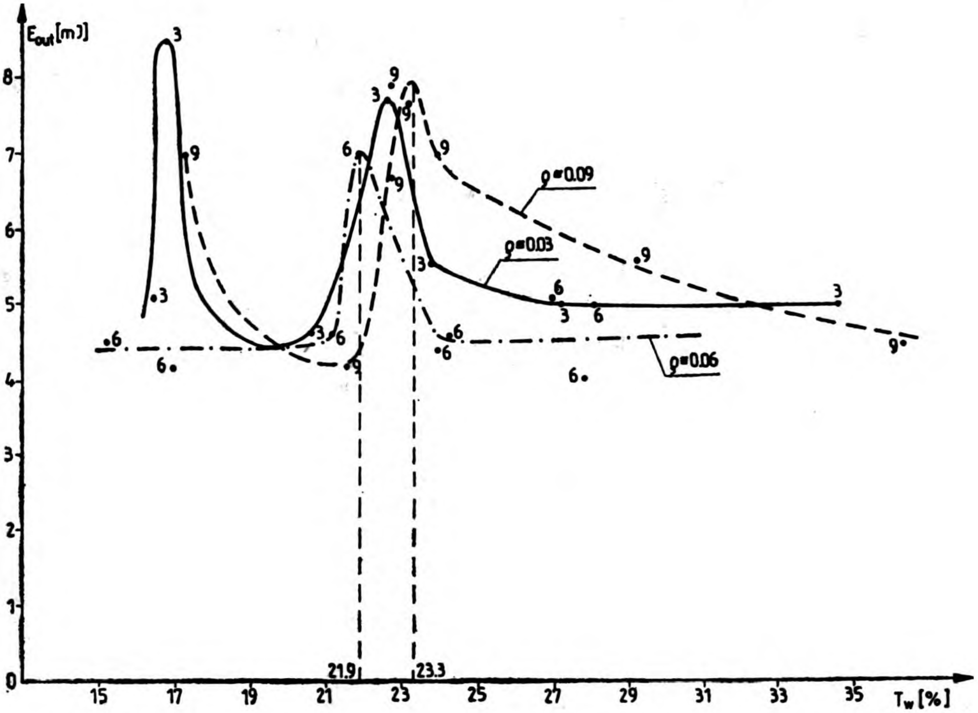

Fig. 8. The dependence of giant pulse energy generation E_{out} on the resultant transmission for rods with different values of ϱ

selected and presented in Table 5. From this Table and plots shown in Fig. 7 it follows that E_{th} of giant pulse generation depends monotonically on the change of T_w for an arbitrary ϱ. For the rods of $\varrho \cong 0.03$ and 0.06 it is observed that the threshold energy grows with T_w, but for the rods with $\varrho \cong 0.09$ this energy decreases with the increasing T_w. The characteristic point is located at the place of the curves intersection (23.5% T_w).

Figure 8 presents the dependence of giant pulse energy generation, E_{out}, on the resultant transmission for rods with different values of ϱ. There are two maximum areas of the generating energy, for $T_w = 17\%$ and 23%, which are independent of the ϱ value.

The dependence of the threshold generation voltage for giant pulse generation on the transmission of FNA for an arbitrary transmissions of mirrors is shown

Table 5

No. of a rod Parameters	65	86	88	93	102	123	141
U_p [V]	870	800	800	855	740	880	870
E_p [J]	4.24	3.58	3.58	4.09	3.07	4.34	4.24
T_w [$^0/_0$]	34.6	20.6	22.7	23.8	16.4	16.8	27.2
E_{out} [mJ]	5.0	4.6	7.7	5.6	5.1	8.5	5.0

No. of a rod Parameters	72	78	82	87	89	90	92	104	105	108
U_p [V]	870	890	840	830	820	720	840	730	740	840
E_p [J]	4.24	4.44	3.95	3.86	3.77	2.90	3.95	2.98	3.07	3.95
T_w [$^0/_0$]	27.0	28.1	21.9	21.2	23.4	24.7	24.0	15.2	17.0	27.8
E_{out} [mJ]	5.1	5.0	7.0	4.6	4.6	5.0	4.4	4.5	4.2	4.0

No. of a rod Parameters	63	98	101	103	124	126	131	135
U_p [V]	870	760	810	780	840	880	870	840
E_p [J]	4.24	3.24	3.67	3.41	3.95	4.34	4.24	3.95
T_w [$^0/_0$]	21.6	36.3	29.2	23.2	17.3	22.8	24.0	22.7
E_{out} [mJ]	4.2	4.5	5.6	7.7	7.0	6.7	7.0	7.9

in Fig. 9. It is seen that for $\varrho \simeq 0.03$ and 0.06 threshold voltage which increases with the FNA transmission is greater for the smaller ϱ. For $\varrho \simeq 0.09$ threshold voltage decreases with the increasing T_f ($C = 11.2$ pF). It is also seen that with the increasing mirror transmission T_s (i.e. (T_w)) generation threshold decreases.

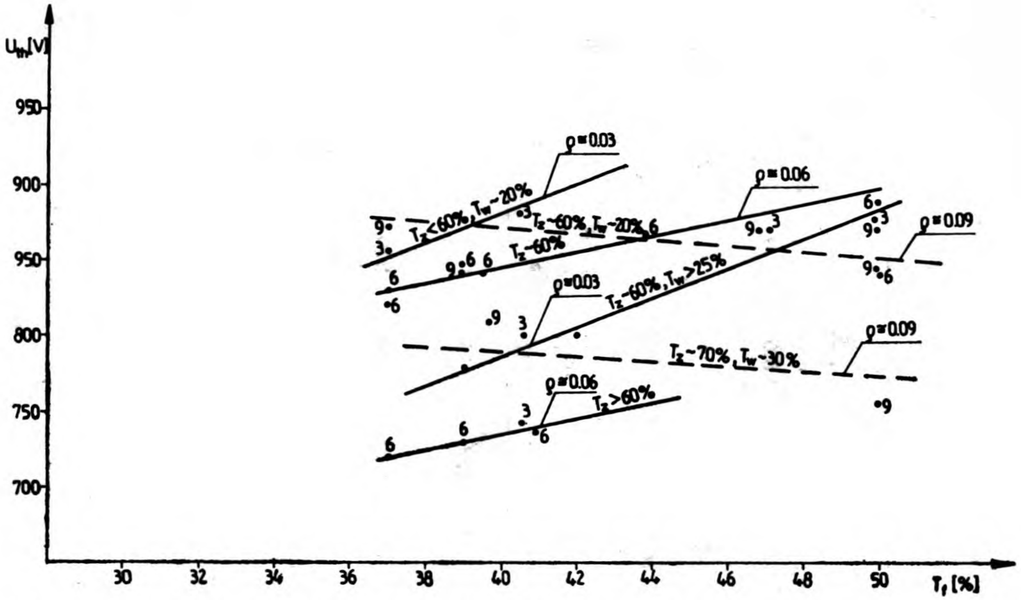

Fig. 9. The dependence of the threshold generation voltage for giant pulse generation on the transmission of FNA for an arbitrary transmissions of mirrors

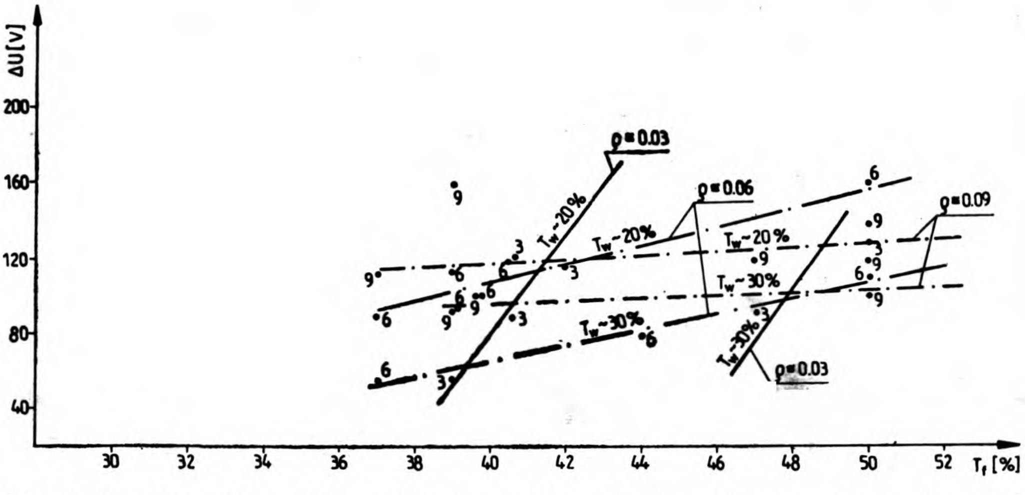

Fig. 10. The dependence of the width of the region of monomode generation on the FNA transmission

Figure 10 presents the dependence of the width of the region of monomode generation on the T_f. It is seen, that for all presented values of ϱ the witdh increases with the increasing T_f and it is greater for smaller ϱ.

Thus, generally, with the increasing FNA transmission the threshold generation energy for the giant pulse generation and the width of the monomode generation region increase while the value of output generation energy decreases. For larger absorption coefficient $\varrho \cong 0.09$ the value of the threshold generation energy decreases with the increasing T_f.

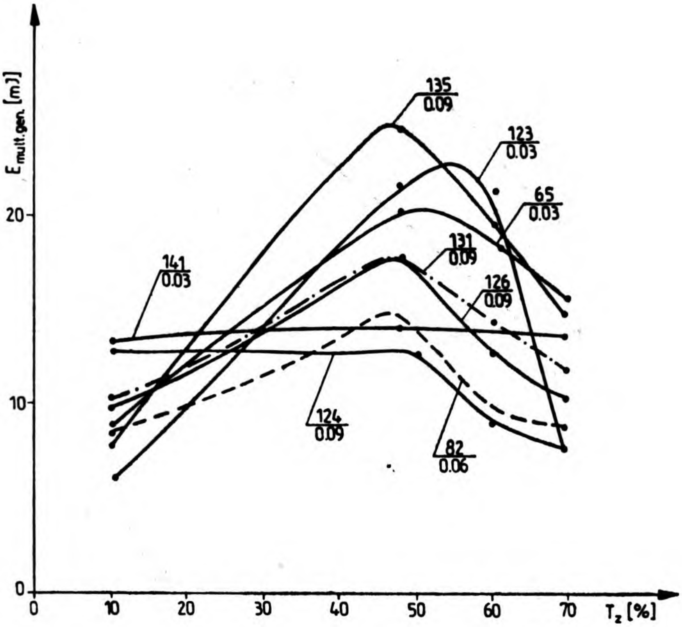

Fig. 11. The dependence of multimode generation energy on the transmission of output mirror

Figure 11 shows the dependence of the multimode generation energy on the transmission of output mirror. It is seen, that it is possible to select the Q-switch for a rod of an arbitrary ϱ. The greatest multimode generation energy cannot correspond (for a given rod) to the greatest output generation energy for the giant pulse generation. For example, from the laser head with the rod No. 124 we have obtained $E_{\text{out}} = 7$ mJ and with the rod No. 135 $E_{\text{out}} = 7.9$ mJ in spite of their just the same ϱ and the maximum of the multimode generation energy differing by $100^{0}/_{0}$. In this figure one can see the two rods of similar characteristics (after selecting Q-switch) and physical properties (131 and 126) and the two rods of the same as previous value of ϱ but of completely different properties of generation (135 and 124). This means that the rods of the same values of ϱ must still differ in one physical parameter at least [3].

Figure 12 provides one more proof for the above. There, the dependence of the pumping voltage U_p(V) on the multimode generation energy is shown, for the $\varrho \simeq 0.03$. It is seen, that for the rods of the same values of ϱ one can obtain the different multimode generation energies in the laser rod.

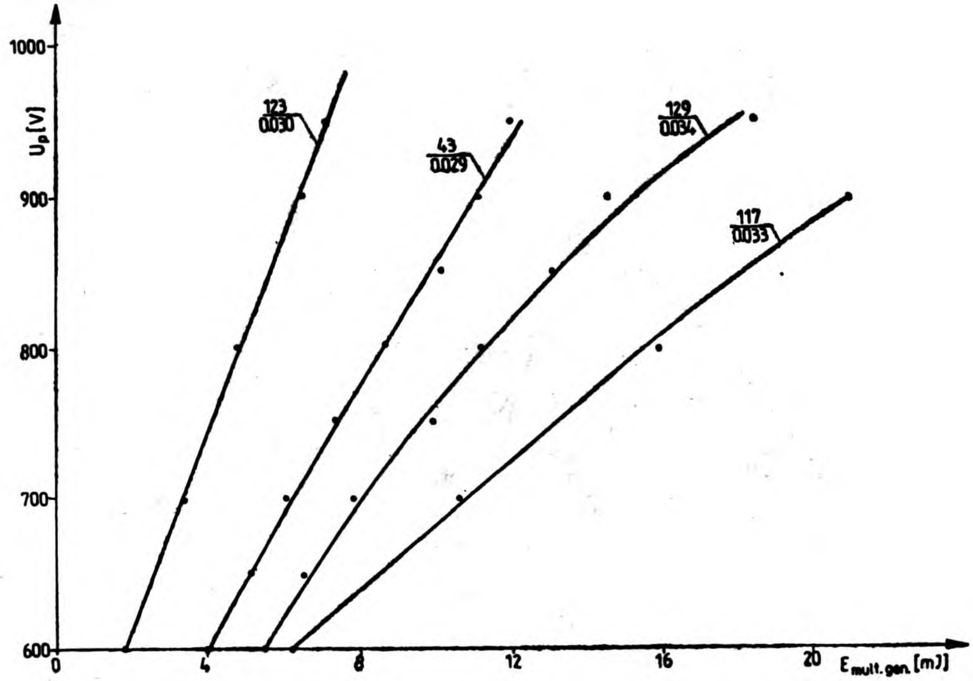

Fig. 12. The dependence of the pumping voltage U_p(V) on the multimode generation energy

6. Influence of absorption coefficient on generation characteristics of laser heads

Figure 13 shows how (after selecting Q-switch) the T_f, T_z and T_w change with the absorption coefficient (ϱ) for the selected rods. It is seen that the conduction of Q-switch (T_w) is determined by the value of T_s independently of $\varrho(T_s^{\nearrow}-T_w^{\nearrow}, T_s^{\swarrow}-T_w^{\swarrow})$. The characteristic maxima may be seen for $\varrho = 0.03$, 0.048, 0.06, 0.08 and 0.096. The maxima may be also observed in the next figures.

Figure 14 shows the dependence of the threshold generation voltage for the giant pulse generation for the laser heads with different rods (different ϱ). The maximal values of threshold voltage appear at the places just between those mentioned above, namely $\varrho = 0.040$, 0.056, 0.070 and 0.092. Thus, a good laser head (a good rod) must have the small value of threshold voltage of giant pulse generation.

In Figure 15 the dependence of width of the appearing monomode generation on the ϱ is shown. Here, we have obtained the confirmation of the preceding result: the better the laser head – the narrower ΔU.

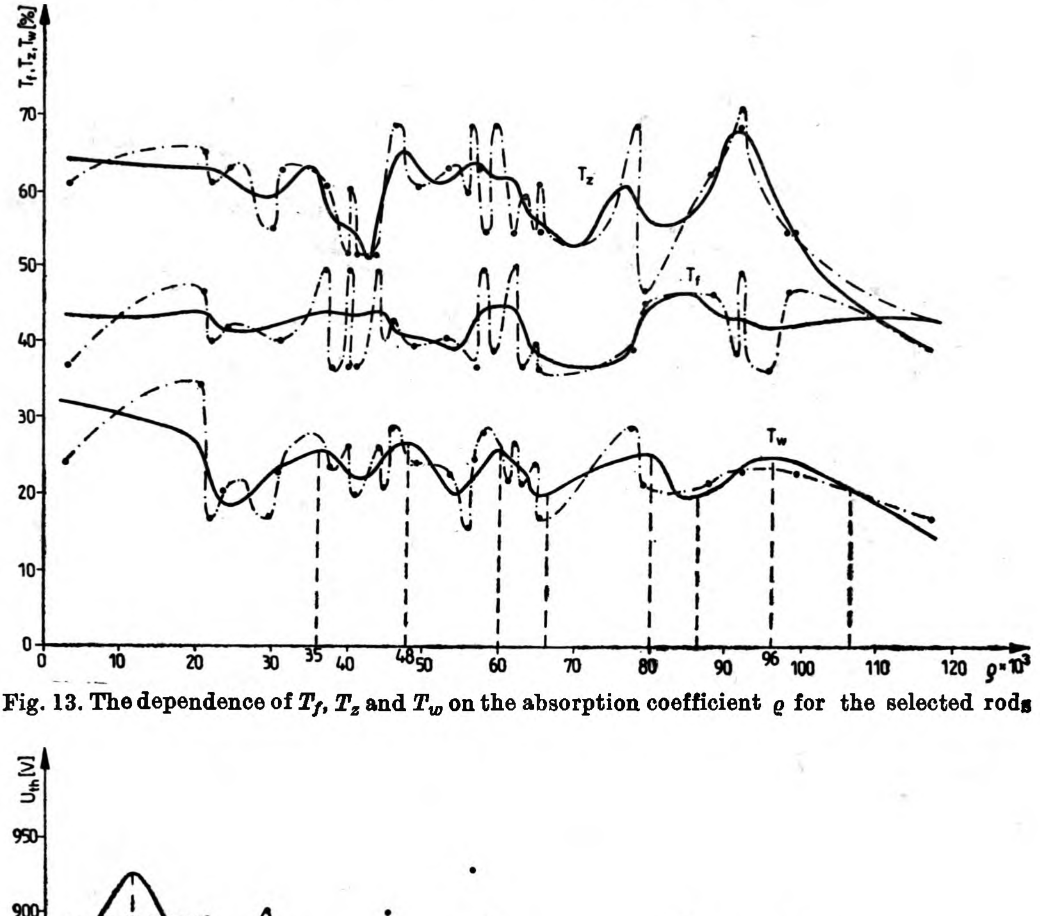

Fig. 13. The dependence of T_f, T_z and T_w on the absorption coefficient ϱ for the selected rods

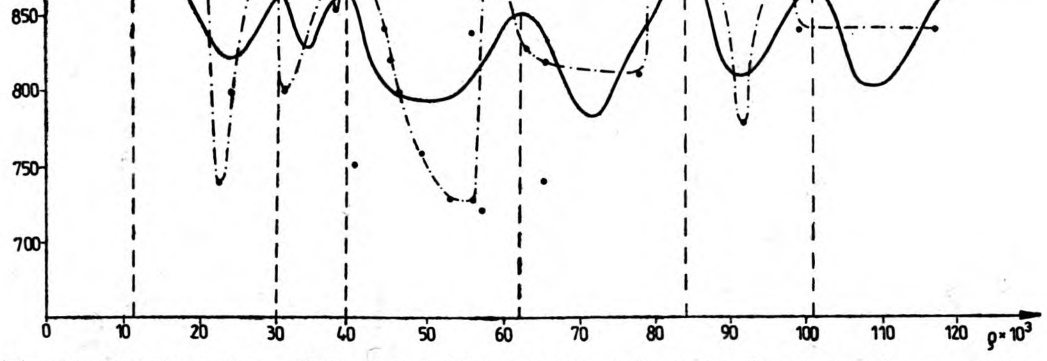

Fig. 14. The dependence of the threshold generation voltage for the giant pulse generation for the laser heads with different rods

Figure 16 presents the dependence of giant pulse generation energy on the ϱ. It is seen that the maximal generation energy appears for the same values of ϱ as shown in Fig. 13. Similar situation may be observed in Fig. 17. In this figure

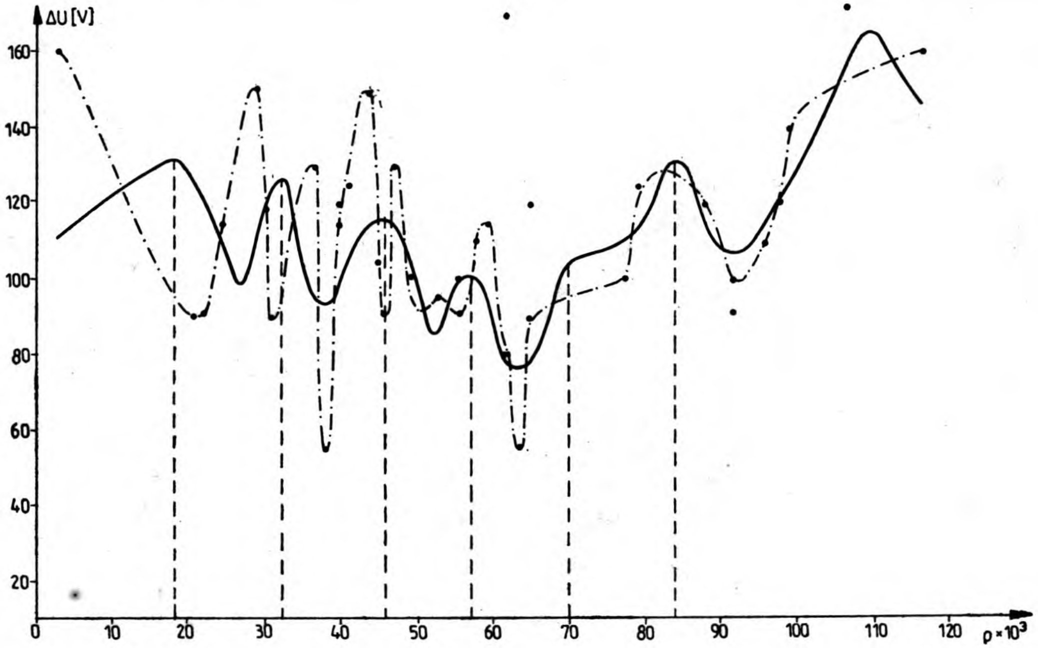

Fig. 15. The dependence of width of the appearing of monomode generation on the absorption coefficient ϱ

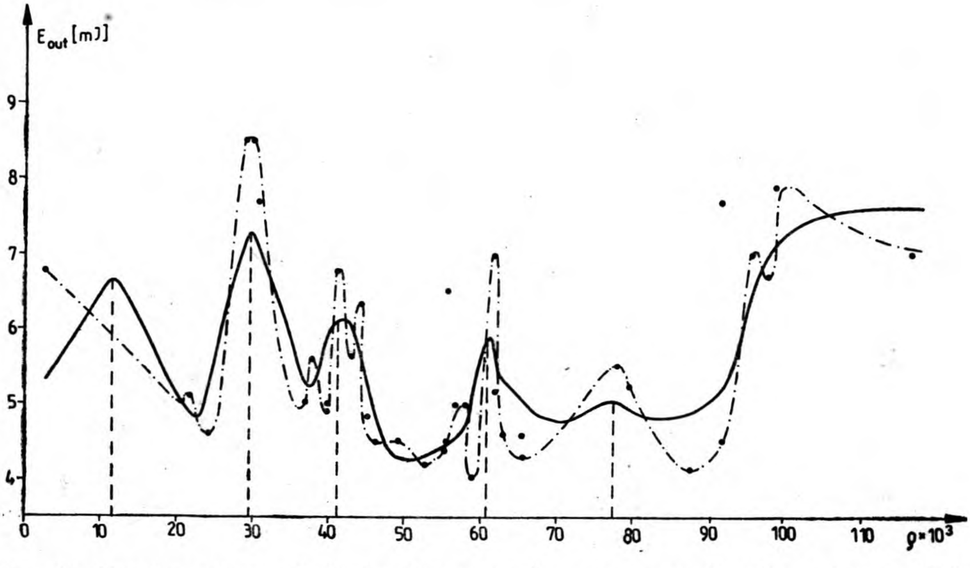

Fig. 16. The dependence of giant pulse generation energy on the absorption coefficient ϱ

the dependence of multimode generation energy on the absorption coefficient ϱ for the pumping voltage 850 V and mirror transmission $T_z = 60.9\%$ is shown.

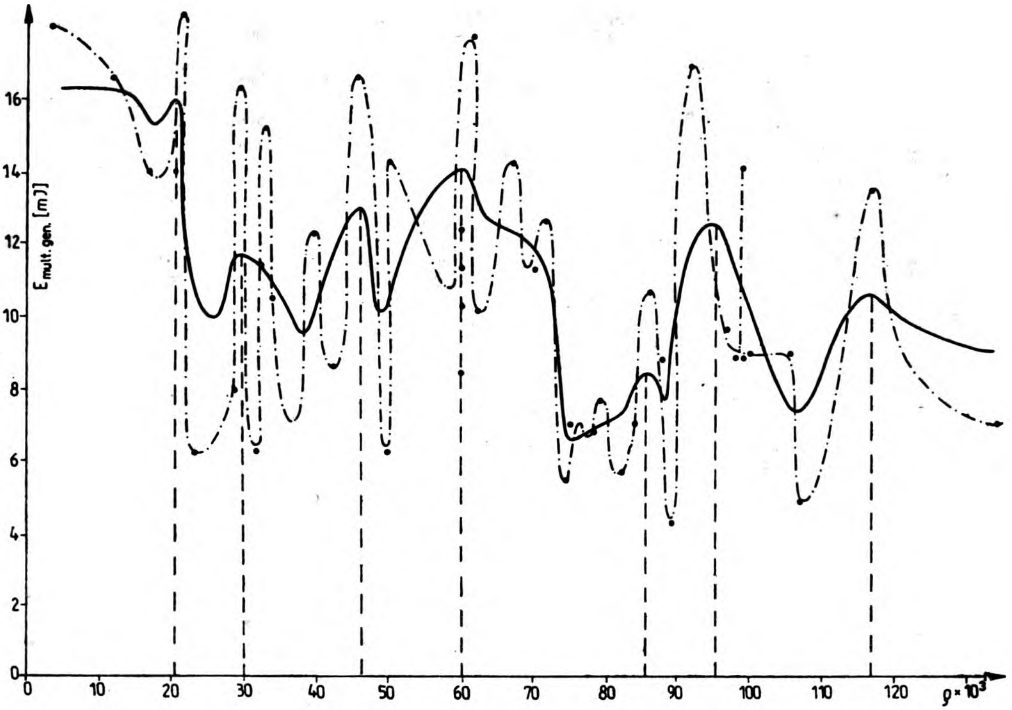

Fig. 17. The dependence of multimode generation energy on the absorption coefficient ϱ for the pumping voltage 850 V and mirror transmission $T_z = 60.9\%$

7. Results

The scatter of the multimode generation energy can be explained by the fact that the position of the rod in the laser head with respect to the optical axis is non optimal. In connection with the change of optical properties of a rod on its cross-section, its rotation by an arbitrary angle around the optical axis causes the change of measured $E_{\text{mult gen}}$ values even by 100%.

Hence, for the explanation of the energetic characteristics of laser heads selected here, it is necessary to measure the laser emission cross-section of rods.

From the above text one can select the following important results:

i) The explicit correlation of optical and generational features of rods applied in the laser heads is seen.

ii) E_p of giant pulse generation behaves monotonically with the change of T_w and T_f for an arbitrary ϱ. For the rods with $\varrho \simeq 0.03$ and $\varrho \simeq 0.06$ the increase of a threshold energy with T_w and T_f is observed, while for the rods with $\varrho \simeq 0.09$ this energy decreases with T_w and T_f.

iii) The width of monomode generation energy region increases with the increasing T_f and the generation energy of giant pulse generation decreases independently of ϱ.

iv) For the rods with the same value of ϱ one can obtain different multimode generation energies in the laser head.

v) The conduction of Q-switch is determined by the value of T_z.

vi) The better the laser head (i.e., rod) the smaller E_p and the narrower ΔU.

References

[1] Hercher A., Appl. Opt. 6 (1967), 947.
[2] Konarski J., Graczyk A., to be published.
[3] Birnbaum M., Tucker A. W., Fincher C. L., J. Appl. Phys. 52 (1981).

Received July 13, 1983